

A Novel Method of Self-Cross-Linking of Syringaldehyde with Activated Methoxy Groups via Cross-Coupling for Lignin-Based Wood Adhesives

Ega Cyntia Watumlawar and Byung-Dae Park*



Cite This: *ACS Omega* 2024, 9, 28167–28175

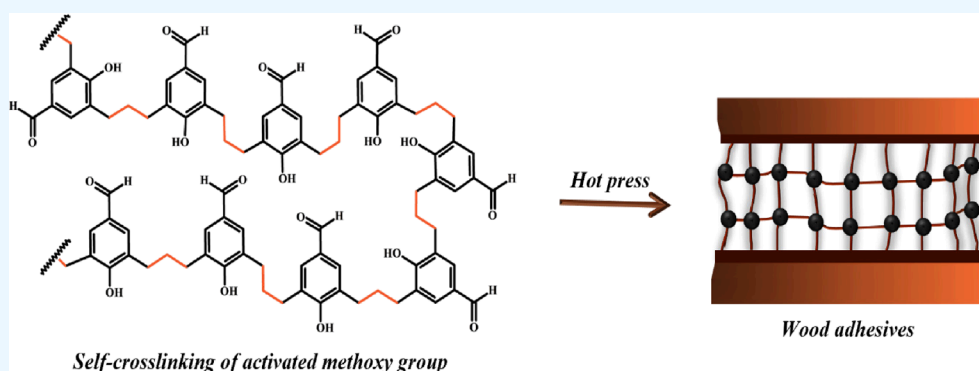


Read Online

ACCESS |

Metrics & More

Article Recommendations



Self-crosslinking of activated methoxy group

Wood adhesives

ABSTRACT: As steric hindrance, methoxy groups are limiting the valorization of hardwood lignin. This paper reports a novel method of self-cross-linking of the syringaldehyde with activated methoxy groups ($-\text{OCH}_3$) via cross-coupling reaction to obtain thermosetting polymers for lignin-based wood adhesives. The methoxy groups of syringaldehyde have been activated via cross-coupling reaction by substituting $\text{Ar}-\text{OCH}_3$ with $\text{Ar}-\text{CH}_2-\text{SiMe}_3$, and dichloromethane, leading to cross-linking via methylene bridges to build a thermosetting polymer. FTIR spectra showed a decrease in the intensity of a $-\text{CH}_3$ and $-\text{OH}$ group, owing to the substitution of the methoxy group. ^{13}C NMR spectra also supported these results with the $-\text{SiMe}_3$ signal that disappeared after the cross-linking reaction. Furthermore, cross-linking between the activated methoxy groups was confirmed with a strong exothermic peak at 130°C , resulting in an increase in the adhesion strength as hot-pressing temperature increased from 160 to 180°C . These results suggest that the cross-linking between the activated methoxy groups of syringaldehyde is an important understanding of valorizing hardwood lignin via building thermosetting polymers for lignin-based adhesives.

1. INTRODUCTION

Various modifications of lignin have been widely investigated for lignin-based wood adhesives.^{1–4} Lignin modification utilizes the main structural units of lignin such as *p*-coumaryl alcohol (H-unit), guaiacyl alcohol (G-unit), and sinapyl alcohol (S-unit).^{5–7} However, a difference in the proportion of structural units is observed between hardwood and softwood lignin (Table 1). Softwood lignin that has a higher proportion of guaiacyl lignin has been investigated by using various modification methods to build lignin-based adhesives. For example, phenolation,^{8–10} demethylation,^{2,11} hydroxymethylation,^{12–14} glyoxalation,^{15,16} and allylation^{5,17–19} have been used to modify softwood lignin and to build a cross-linked network with three-dimensional linkages for the synthesis of adhesives. However, hardwood lignin with a high proportion of the syringyl unit is known as a weakness to create a cross-linked network structure due to the less reactive methoxy group in the unit.²⁰ In recent studies, hardwood lignin

modifications have been mainly based on exploiting their *para* and *ortho* positions.^{7,21} Thus, a novel approach for the *meta* position of aromatic hardwood lignin was noticed for this study.

The methoxy group is a functional group that contains a methyl group bound to oxygen and has high application potential in the medical field^{23,24} but not in the adhesive application. The methoxy group has been utilized as a protecting group in many substrates.^{25–28} Moreover, the methoxy groups of lignin have been used to prepare amides via carbonylation²⁹ and have been converted to obtain pure

Received: February 8, 2024


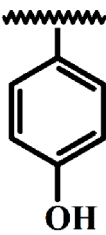
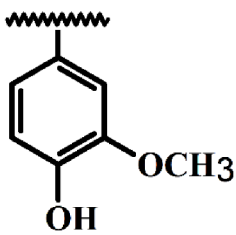
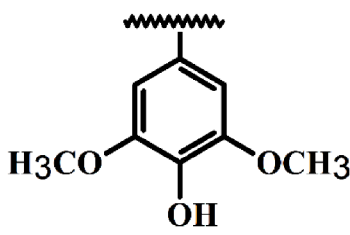
Revised: June 2, 2024

Accepted: June 11, 2024

Published: June 20, 2024



Table 1. Proportion of the Structural Units in Hardwood and Softwood Lignin

	H-unit (%)	G-unit (%)	S-unit (%)
 Lignin			
Hardwood*	<8	20–60	40–75
Softwood	<10	>95	2–3

*The data was cited from ref 22.

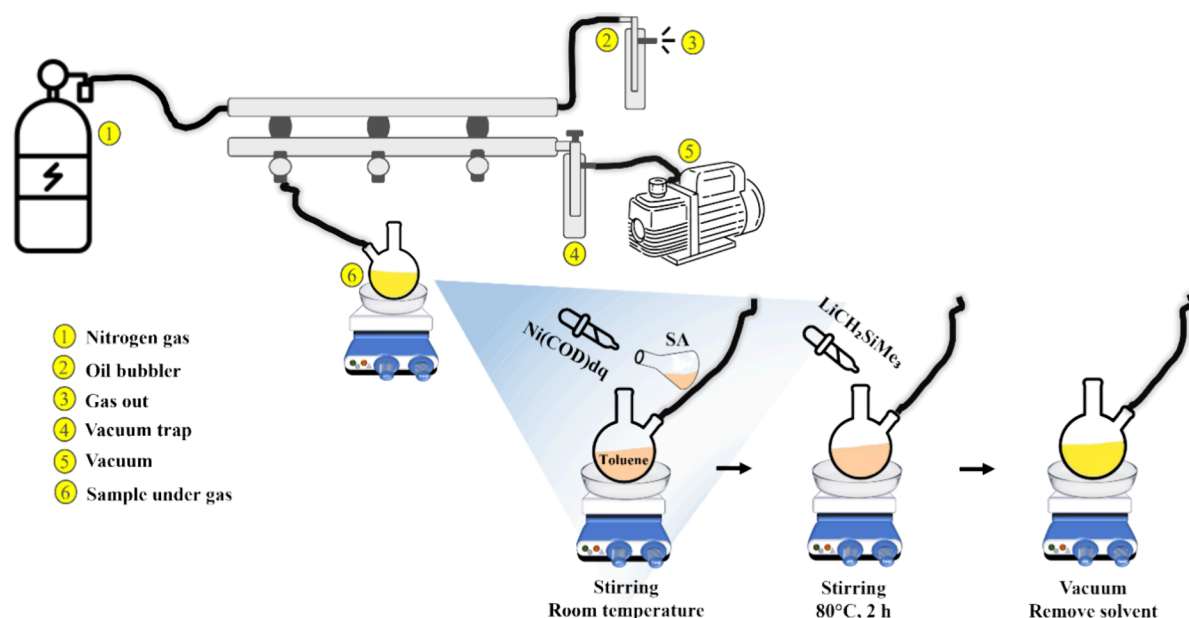


Figure 1. Schematic diagram of the reaction setup for the activation of the methoxy group of SA under nitrogen gas.

chemicals.³⁰ However, the modification of the methoxy group with a substitution method has become a promising alternative strategy.³¹ The substitution of the methoxy group has been conducted to produce cyclized products via *ipso* substitution through nucleophilic and electrophilic aromatic substitutions.^{25,32} Furthermore, a substitution via cross-coupling reaction has attracted considerable interest because of the potential reaction of substrate and reagent with the aid of a catalyst under mild conditions.³¹ Previous studies employed cross-coupling reactions for the synthesis of several chemicals to incorporate an alkyl group into aromatic rings with metal-catalyzed cross-coupling,³³ to synthesize two chemical compounds with the addition of organometallic species,³⁴ and to substitute the methoxy group.^{31,35} However, the activation of methoxy groups of syringaldehyde (SA) via cross-coupling reaction has not been reported yet for the self-cross-linking of SA. This methoxy group activation makes it possible to generate activated carbon atoms of the methoxy groups of SA for their self-cross-linking to build a network structure as adhesives.³¹

SA is a naturally occurring compound with various bioactive characteristics that occur in lignin.³⁶ Lignin provides a continuous, renewable, and cheap supply of SA.³⁷ Hence, the SA model compound is a potential lignin compound with a methoxy group in two *meta* positions, due to numerous studies of SA depolymerization from lignin with stable conditions and high yield.³⁸ SA has been studied for its biological effects using a semisynthetic method,³⁹ and the excellent performance of SA has indicated the application potential of this compound in thermoset polymer.^{40–42}

The objectives of this work are to activate the methoxy groups of the SA model compound and to cross-link the activated SA to build thermosetting polymers with a network structure as lignin-based adhesives for bonding wood. Thus, this study investigated a novel method of self-cross-linking through the activation of methoxy groups and their cross-linking to build a network structure by forming methylene bonds.

Scheme 1. Schematic Reactions of the Activation of Methoxy Groups of SA

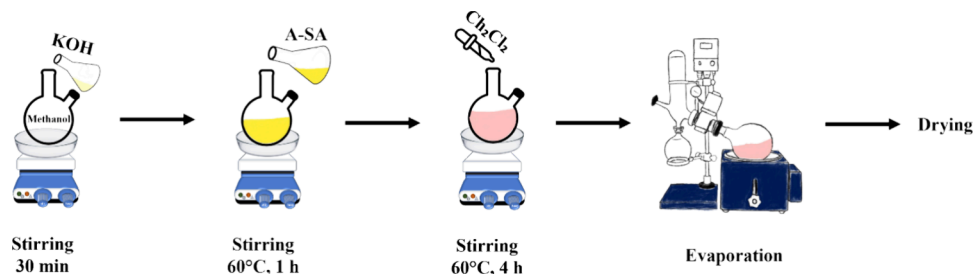
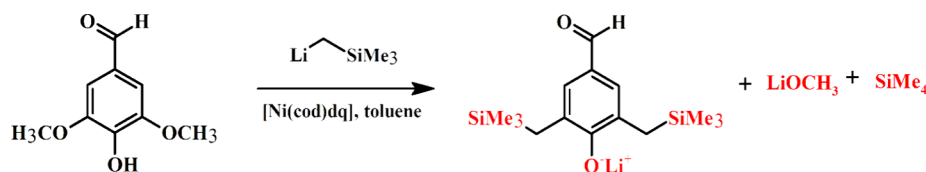
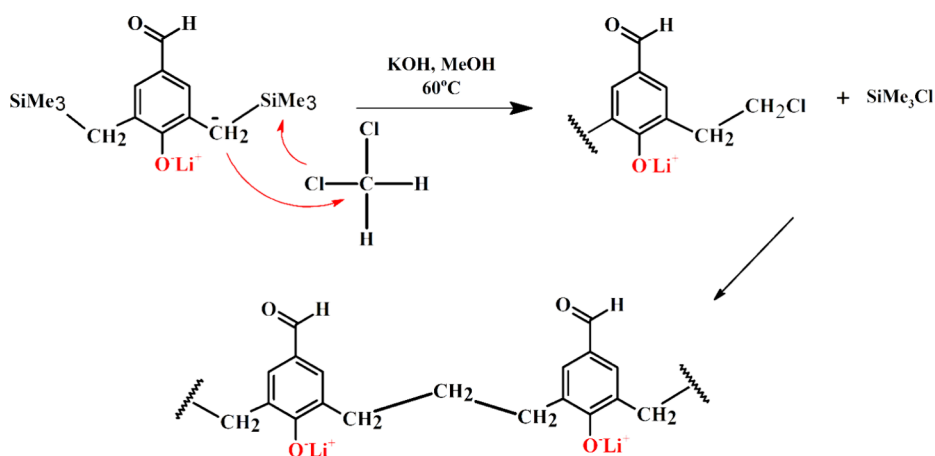


Figure 2. Schematic procedures of the self-cross-linking of A-SA.

Scheme 2. Self-Cross-Linking Reaction of SA with the Activated Methoxy Groups



2. MATERIALS AND METHODS

2.1. Materials. The SA model compound and Ni(COD)dq were obtained from Sigma-Aldrich, USA. $\text{LiCH}_2\text{SiMe}_3$ and toluene were purchased from Thermo Fisher Scientific, USA. Methyl alcohol (methanol) was obtained from Duksan Chemical, Korea. Potassium hydroxide (KOH), dimethyl sulfoxide (DMSO), and dichloromethane (DCM) were obtained from Daejung Chemicals, Korea.

2.2. Methods. **2.2.1. Synthesis of the Activated Methoxy Group of SA.** The method used for synthesizing the methoxy group of SA was adapted from the method published in the literature;³¹ the method is schematized in Figure 1. An oven-dried, nitrogen-flushed Schlenk tube was charged and was ready to use. First, 52 mg of SA (0.279 mmol) and 0.926 mg of Ni(COD)dq (1 mol %) were added in the tube. Subsequently, the tube was immediately sealed and flushed with nitrogen. Thereafter, 1.5 mL of toluene and 1.178 mL of a $\text{LiCH}_2\text{SiMe}_3$ solution in hexane (0.7 M, 3.3 equiv) were added and the mixture was stirred for 2 h at 80 °C. The activated SA (A-SA) product was vacuumed to remove the solvent and then characterized.

In this study, an SA model compound with two methoxy groups in the *meta* position was reacted with activated Li and nickel catalysts, where a cross-coupling reaction might have occurred. In addition, the reaction with $-\text{OH}$ groups also

occurred during the activation. However, the product is expected to substitute for $-\text{OCH}_3$ and activate it into $-\text{CH}_2-\text{SiMe}_3$ (Scheme 1).

2.2.2. Self-Cross-Linking of SA with the Activated Methoxy Groups. Initially, 10 mL of 1 N KOH solutions was prepared in a round-bottom flask and mixed with 20 mL of methanol for 30 min under room temperature. Subsequently, 546.5 mg of A-SA was added to the flask and the mixture was stirred for 1 h at 60 °C. Thereafter, 2 mL of DCM was added slowly, followed by stirring at 60 °C for 4 h. The mixture was evaporated under a vacuum to remove the solvent before being analyzed. The procedure is shown in Figure 2.

In addition, further modification to accomplish cross-linking between substrates can occur via self-cross-linking. We developed a new reaction in the form of self-cross-linking to build a methylene bridge among activated products. Dichloromethane (DCM) functioned as a reagent to afford a methylene bridge among activated products (Scheme 2). Fourier transform infrared (FTIR) spectroscopy, ^{13}C nuclear magnetic resonance (^{13}C NMR) spectroscopy, and thermal behavior analysis were performed to investigate self-cross-linking of A-SA molecules.

2.2.3. FTIR Spectroscopy. The functional groups of SA, A-SA, and cross-linked SA (C-SA) after the cross-linking reaction were characterized via attenuated total reflectance infrared



Figure 3. Samples of (a) syringaldehyde (SA), (b) activated syringaldehyde (A-SA), and (c) self-cross-linked SA (C-SA).

spectroscopy (ALPHA, Bruker Optics GmbH, Ettlingen, Germany). The FTIR spectra were recorded in the 4000–400 cm^{-1} range with a resolution of 4 cm^{-1} and 32 scans.

2.2.4. Differential Scanning Calorimetry (DSC). A DSC instrument (Discovery 25, TA Instruments, New Castle, USA) was used to determine the thermal behavior of SA, A-SA, and C-SA. A dried sample (3–5 mg) was sealed in an aluminum pan with a lid. The samples were equilibrated for 30 min and then heated to 250 $^{\circ}\text{C}$ at a rate of 10 $^{\circ}\text{C}/\text{min}$ under a nitrogen flow of 50 mL/min.

2.2.5. Solid-State ^{13}C NMR Spectroscopy. Solid-state ^{13}C cross-polarization/magic-angle-spinning (CP/MAS) NMR spectra were acquired using NMR spectroscopy (Bruker Avance III HD, Rheinstetten, Germany; 400 MHz) to characterize the chemical structure of all samples.⁴³ The powder sample was investigated using a 4 mm CP-MAS probe at a frequency of 100.6 MHz and a spinning rate of 10 kHz. Thus, structural information that could not be obtained via infrared spectroscopy was addressed.

2.2.6. Determination of Adhesion Strength. The adhesion strength was determined at room temperature using a Universal Testing Machine (OTT-005, Oriental TM, Republic of Korea). The test was carried out with thin rectangular wood strips (30 mm wide \times 30 mm long), and adhesives were spread over the overlapping area (10 mm \times 10 mm) with 400 g/ m^2 glue spread. Then, the bonded wood stripes were hot-pressed at 160 or 180 $^{\circ}\text{C}$ for 8 min. The lap shear specimens were tested in tensile conditions at a crosshead speed of 0.5 mm/s. At least three replicates were tested for each sample, and their average values were reported.

3. RESULT AND DISCUSSION

The synthesis of the methoxy group of SA and self-cross-linking reaction have succeeded providing outcomes. Cross-coupling reactions in the form of oxidative addition, transmetalation, and reductive elimination might be assumed to have occurred in the transformation between $-\text{OCH}_3$ into activated $-\text{SiMe}_3$. The reaction of $\text{LiCH}_2\text{SiMe}_3$ as an activating agent with the methoxy group of SA in the presence of a nickel catalyst has occurred in this study. Certainly, the concentration of reactants, temperature, and the presence of catalysts influence the reaction rates. Temperature is influential because of sufficiently energetic collisions among reactants. Moreover, Figure 3 shows color transformations in each synthesis. SA manifested in the form of a white cream, while the color of A-SA changed to yellow. Furthermore, the self-cross-linking of C-SA displayed a change to orange. The color change during chemical reactions commonly occurs probably because of the changes in energy emitted by the electron while the reaction occurs.^{44,45}

In addition, DCM has been selected as a solvent in various organic applications.^{46–48} As a reagent, DCM has shown a

good performance. During electron bond formation, DCM reacted by acquiring electrons or sharing electrons that previously belonged to A-SA⁴⁹ (Scheme 2). The activation of DCM has been studied to build methylene-bridged bisamines, which are usually used as ligands in chemical applications.⁵⁰ In addition, DCM has been used in combination with pyridine under ambient conditions.⁵¹ DCM has also been used as a reagent in the synthesis of pyrrole to obtain high yields under phase-transfer conditions.⁵² The methylene bridge that formed during the A-SA reaction provides a self-cross-linking reaction that could generate cohesion for adhesives. Therefore, chemical analyses were conducted.

3.1. FTIR Spectroscopy. FTIR analysis was conducted to understand the substitution of the functional methoxy groups of SA, A-SA, and C-SA. Table 2 shows the SA spectra consisting of a common linkage, as reported in the literature.⁵³ Figure 4 shows that transformations among spectra have occurred during every reaction. Substituting the methoxy

Table 2. FTIR Band Assignment of SA

wavenumber (cm^{-1})	vibration assignments ^a
3250	ν OH and CH
3032	ν_{as} CH_3
2967, 2940	ν CH , ν_{s} CH_3
2863, 2838	ν_{s} CH_3
1667	ν $\text{C}=\text{O}$, ν CC
1606	ν CC
1583	ν CC
1511	δ_{as} CH_3
1451	δ_{as} CH_3 , β CH
1422	δ_{s} CH_3 , β CH
1403	ν CC, β CH
1366, 1327	ν CC, δ_{s} CH_3 , β CH
1277	ν CO, β CH, δ_{s} CH_3
1249	ν CO, β CH, β OH
1202	β OH, β CH
1137	ν CO, β CH
1099	ν CO, β CH
1036	ν CO, β CH
907	γ CH
828	γ CH
767	γ CH, δ C–OH, δ_{as} CH_3
723	γ CH, γ OH
665	γ OH, δ C–OH, δ_{as} CH_3
633	γ OH, δ C–OH, δ_{as} CH_3
583	γ OH
522	γ OH, δ C–OH

^a ν , stretching; ν_{s} , symmetric stretching; ν_{as} , asymmetric stretching; δ , bending; δ_{s} , symmetric bending; δ_{as} , asymmetric bending; β , in-plane bending; γ , out-of-plane bending.

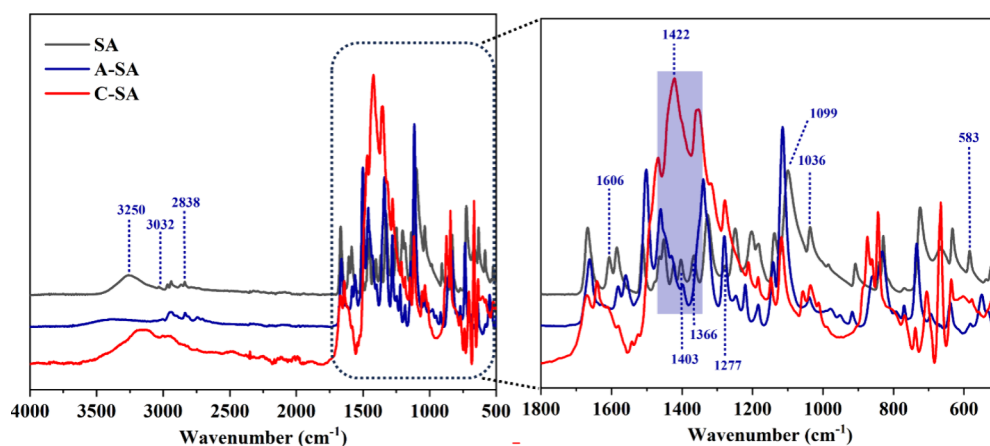


Figure 4. FTIR spectra of SA, A-SA, and C-SA.

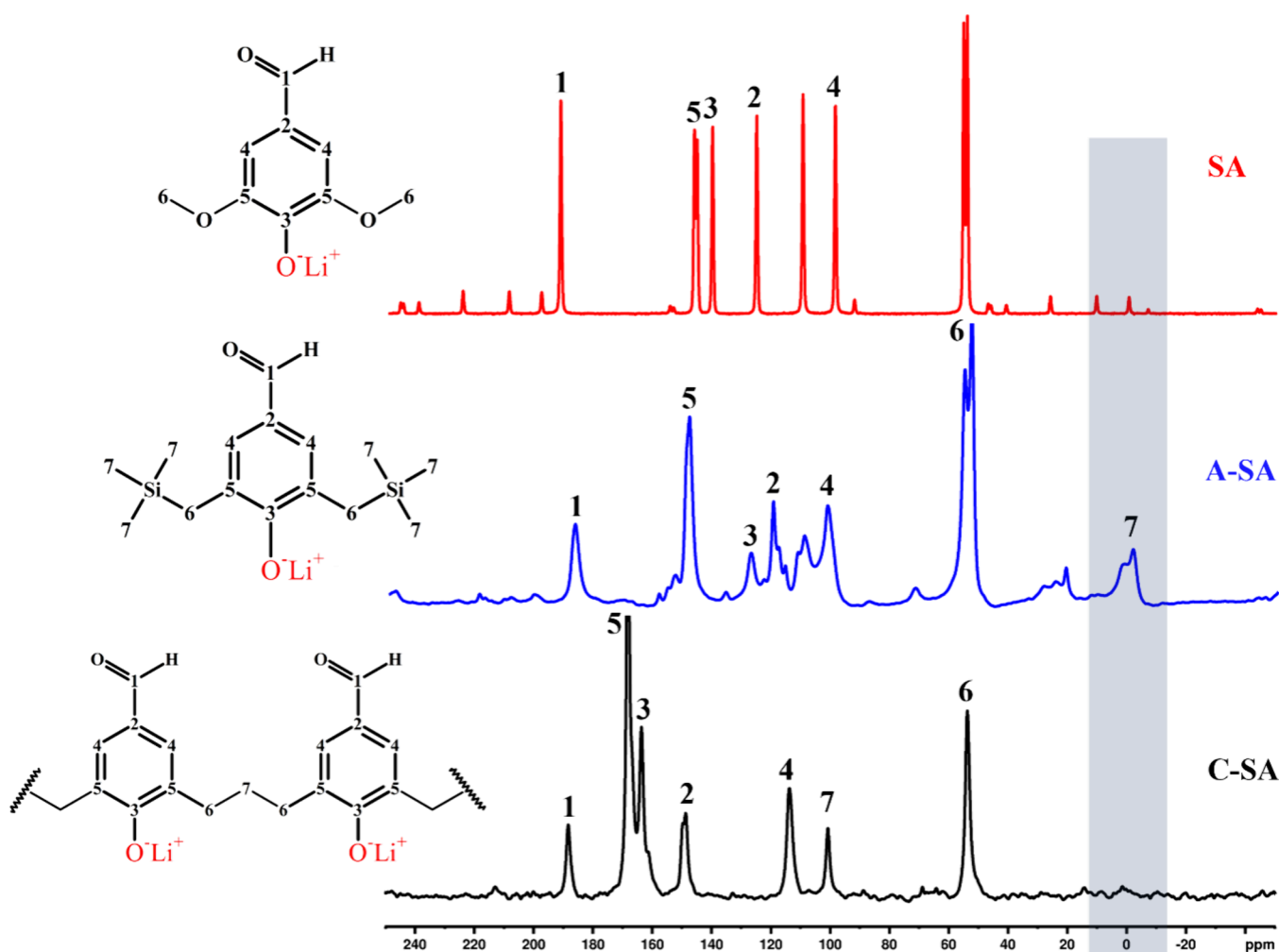


Figure 5. ^{13}C CP/MAS NMR spectra and chemical structures of SA, A-SA, and C-SA.

group with $\text{LiCH}_2\text{SiMe}_3$ revealed the disappearance of peaks from the A-SA spectra, particularly those belonging to $-\text{OCH}_3$ at 1277 cm^{-1} . Furthermore, after methoxy group activation, C-SA exhibits other peaks, such as those at 1403 and 1366 cm^{-1} , indicating a reduction in the spectral intensity of the C–C reaction. However, an interesting phenomenon has shown that the band intensities at 3250 cm^{-1} corresponding to $-\text{OH}$ of A-SA have decreased. This result indicates that $\text{LiCH}_2\text{SiMe}_3$

reacts with $-\text{OH}$ groups and is converted to O^-Li^+ , besides the methoxy groups. Moreover, the self-cross-linking reaction indicated that two molecules of A-SA serve as a nucleophile and DCM serves as an electrophile to combine and form a single molecule that builds a methylene bridge. During the reaction, water is usually released as a secondary product. In addition, the Si–C network suggests that incorporation is formed with a large amount of H.⁵⁴ Therefore, the spectra of

A-SA at 2940 cm^{-1} corresponding to $-\text{CH}$ indicates the possible occurrence of $\text{Si}-\text{CH}_3$ stretching.⁵⁴

Based on the self-cross-linking of A-SA, Figure 4 shows the FTIR spectra of C-SA. The activated methoxy group and the $-\text{CH}_2-\text{SiMe}_3$ network led to the formation of a methylene bridge via a reaction between $-\text{CH}_2-$ groups and $-\text{CH}_2^+$ of CH_2Cl_2 under room temperature, causing the reaction to accelerate and cause cross-linking to form a polymer–particle network. The graph revealed that the self-cross-linking of C-SA might have succeeded by the presence of a 1422 cm^{-1} band known as the methylene bridge.

3.2. ^{13}C NMR Spectral Analysis. ^{13}C CP/MAS NMR analysis was conducted to investigate the chemical spectra of SA, A-SA, and C-SA. Figure 5 shows SA's chemical shifts, whereas the number of chemical shift assignments is shown in Table 3. The SA shows the chemical shifts that are corresponding well with the peaks reported in the literature.⁵³

Table 3. Chemical Shift Assignments of ^{13}C NMR Spectra

sample	peak number	δc (ppm)
SA	1	192.23
	2	126.01
	3	140.91
	4	99.33
	5	146.61
	6	55.19
A-SA	1	187.45
	2	120.49
	3	128.03
	4	102.09
	5	148.82
	6	55.74
	7	0.37
C-SA	1	188.55
	2	149.19
	3	163.72
	4	113.87
	5	168.33
	6	53.90
	7	100.81

Furthermore, NMR provides precise information about the interatomic interaction that cannot be obtained using other structural techniques.^{55,56} SA shifts are for the alkyl groups (0–50 ppm), O-alkyl groups (50–110), aromatic groups (110–165 ppm), and carbonyl groups (165–200 ppm).^{57,58} In particular, the spectra of A-SA and C-SA revealed peak changes corresponding to alkyl groups. A-SA exhibited a new peak around $\delta = 0.37\text{ ppm}$ attributed to the $\text{Si}-\text{Me}_3$ linkage. However, the results confirmed that corrosion after synthesis might occur, as made evident by the reduction of spectral intensity. A catalyst of high activity might affect degradation and discoloration.⁵⁹ The self-cross-linking reaction of C-SA can build a methylene bridge between $-\text{CH}_2-\text{SiMe}_3$ of the C-SA and CH_2Cl_2 of DCM. Spectral analysis of C-SA has proven the disappearance of the $-\text{SiMe}_3$ linkage in $\delta = 0\text{ ppm}$; instead, a new strong peak showed around $\delta = 100.81\text{ ppm}$, indicating that a new linkage has formed, which could serve as a methylene bridge.

3.3. Thermal Behavior Using DSC. Thermal behaviors of SA, A-SA, and C-SA were investigated using DSC. DSC analysis detects thermal transitions that display endothermic or

exothermic peaks in a sample. In other words, this analysis monitors heat-induced phase transition changes that determine the temperature and heat flow associated with the material transition as a function of time and temperature, respectively.⁶⁰ In polymers, a phase transition has been studied to understand the relationship between properties and microstructure.⁶¹ Furthermore, in the case of thermoset polymers, DSC measurement is important to understand the phase transition of cross-linking and the curing temperature and time.⁶² As shown in Figure 6a, the SA has a strong endothermic peak starting at approximately $106\text{ }^\circ\text{C}$, indicating the melting process that occurred in SA. This result is compatible with the reported result that the SA-based polymer showed an endothermic peak of SA.³⁷ Moreover, lignin with the methoxy group has considerably lower melting temperatures.⁶³ However, the A-SA reaction involving a nickel catalyst showed an endothermic peak at approximately $40\text{ }^\circ\text{C}$ (Figure 6b), which is decreased compared to that of SA before modification. The activation of the methoxy group has indicated the changes in thermal properties. The endothermic peak of A-SA revealed the melting process, indicating that decomposition might have occurred during the reaction. However, partial crystallization at approximately $108\text{ }^\circ\text{C}$ might have occurred.

Furthermore, the self-cross-linking reaction of C-SA (Figure 6c) has been proven by the presence of a strong exothermic peak at approximately $130\text{ }^\circ\text{C}$. The C-SA peak indicated that such cross-linking has developed after the reaction. However, the self-cross-linking reaction has been confirmed by the presence of a new peak in FTIR and ^{13}C -NMR. The formation of a methylene bridge can occur by causing reactions between $-\text{CH}_2-\text{OH}$ groups and $-\text{CH}_2^+$ groups under ambient conditions where it will start to grow and cross-link to form a polymer–particle network.⁶⁴ The result of C-SA showed the potential to cross-link A-SA with DCM as a reagent.

4. ADHESION STRENGTH

To evaluate the adhesive strength of the novel path of SA self-cross-linking, C-SA has been tested for lap shear strength in the thin wooden board. Figure 7 shows the lap shear adhesion strengths of A-SA and C-SA at different hot-pressing temperatures of 160 and $180\text{ }^\circ\text{C}$, as shown in Table 3. However, the hot-pressing temperatures were selected on the basis of the exothermic temperature displayed in DSC. Ten lap shear adhesion strengths gradually increased from 0.07 to 0.12 MPa when the hot-pressing temperature increased from 160 to $180\text{ }^\circ\text{C}$. The results suggest that the cross-linking of the C-SA sample is advanced further in the curing process at a high hot-pressing temperature. Regardless of the adhesion performance, these results provided evidence for the self-cross-linking of C-SA for lignin-based wood adhesives, which is a new way of cross-linking of SA by the activation of its methoxy groups. In addition, the self-cross-linking of C-SA could be improved under higher hot-pressing temperatures in the future.

5. CONCLUSIONS

The results of this study show a novel way of self-cross-linking of SA by activating the methoxy group of SA for lignin-based wood adhesives. After the activation reaction induced a change in its color changes, functional group analysis such as FTIR of SA has shown reduction spectra corresponding to peaks of $-\text{OCH}_3$, indicating the occurrence of methoxy modification of

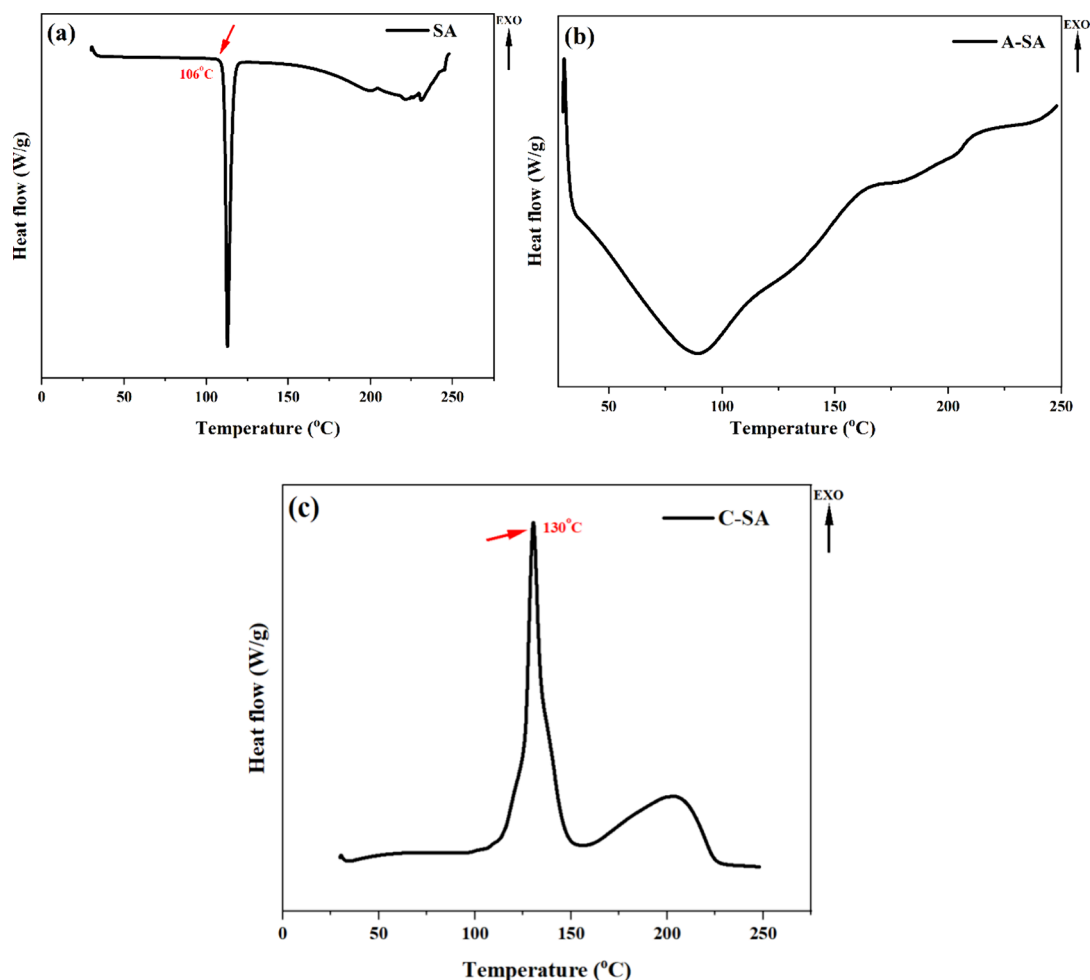


Figure 6. A DSC thermograms of (a) SA, (b) A-SA, and (c) C-SA.

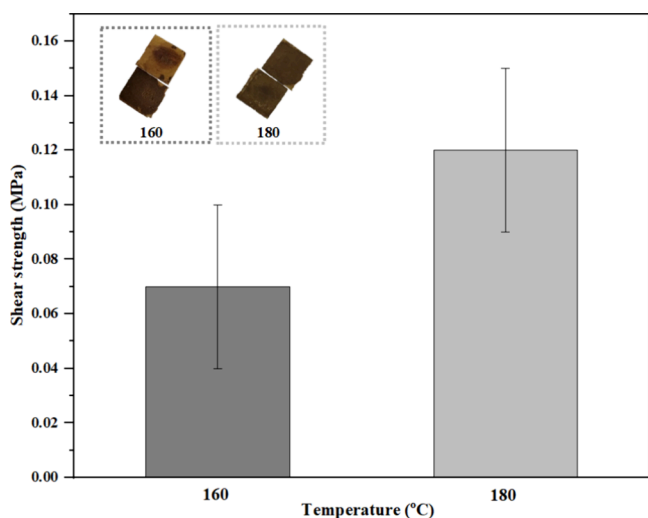


Figure 7. Shear strength and fractured specimens of C-SA.

activated syringaldehyde (A-SA). The A-SA results were supported by chemical structure analysis of the ^{13}C -NMR spectrum that revealed the appearance of a peak belonging to $-\text{SiMe}_3$; this peak disappeared after the self-cross-linking reaction. In addition, the characterization of thermal behavior via DSC has revealed the appearance of a strong exothermic peak around 130 °C after the A-SA reaction, which led to a

cross-linking reaction. The cross-linking reaction was strengthened with adhesion strength as the temperature increased from 160 to 180 °C. This study has opened a new path to develop a novel approach of methoxy groups for creating lignin-based adhesives. Thus, the results could lead to employment of the cross-linking method of hardwood lignin for the application of advanced wood adhesives in the future.

AUTHOR INFORMATION

Corresponding Author

Byung-Dae Park — Department of Wood and Paper Science, Kyungpook National University, Daegu 41566, Republic of Korea; orcid.org/0000-0002-9802-7855; Email: byungdae@knu.ac.kr

Author

Ega Cynthia Watumlawar — Department of Wood and Paper Science, Kyungpook National University, Daegu 41566, Republic of Korea

Complete contact information is available at: <https://pubs.acs.org/10.1021/acsomega.4c01267>

Notes

The authors declare no competing financial interest.

ACKNOWLEDGMENTS

This work was supported by the National Research Foundation (NRF) of Korea, funded by the Korean Government (MSIT) (Grant No. RS-2023-00240043)

REFERENCES

- (1) Yang, S.; Wen, J. L.; Yuan, T. Q.; Sun, R. C. Characterization and Phenolation of Biorefinery Technical Lignins for Lignin-Phenol-Formaldehyde Resin Adhesive Synthesis. *RSC Adv.* **2014**, *4* (101), 57996–58004.
- (2) Song, Y.; Wang, Z.; Yan, N.; Zhang, R.; Li, J. Demethylation of Wheat Straw Alkali Lignin for Application in Phenol Formaldehyde Adhesives. *Polymers* **2016**, *8* (6), 209.
- (3) Aziz, N. A.; Latip, A. F. A.; Peng, L. C.; Latif, N. H. A.; Brosse, N.; Hashim, R.; Hussin, M. H. Reinforced Lignin-Phenol-Glyoxal (LPG) Wood Adhesives from Coconut Husk. *Int. J. Biol. Macromol.* **2019**, *141*, 185–196.
- (4) Gadhave, R. V.; Kasbe, P. S.; Mahanwar, P. A.; Gadekar, P. T. Synthesis and Characterization of Lignin-Polyurethane Based Wood Adhesive. *Int. J. Adhes. Adhes.* **2019**, *95*, No. 102427, DOI: 10.1016/j.jadhadh.2019.102427.
- (5) Jawerth, M.; Lawoko, M.; Lundmark, S.; Perez-Berumen, C.; Johansson, M. Alkylation of a Lignin Model Phenol: A Highly Selective Reaction under Benign Conditions towards a New thermoset Resin Platform. *RSC Adv.* **2016**, *6* (98), 96281–96288.
- (6) Gioia, C.; Colonna, M.; Tagami, A.; Medina, L.; Sevastyanova, O.; Berglund, L. A.; Lawoko, M. Lignin-Based Epoxy Resins: Unravelling the Relationship between Structure and Material Properties. *Biomacromolecules* **2020**, *21* (5), 1920–1928.
- (7) Watumlawar, E. C.; Park, B. D. Synthesis of Acetone-Fractionated Hardwood Kraft Lignin-Based Adhesive Crosslinked with Epichlorohydrin. *J. Adhes. Sci. Technol.* **2024**, *38* (3), 442–457.
- (8) Thébault, M.; Kutuzova, L.; Jury, S.; Eicher, I.; Zikulnig-Rusch, E. M.; Kandelbauer, A. Effect of Phenolation, Lignin-Type and Degree of Substitution on the Properties of Lignin-Modified Phenol-Formaldehyde Impregnation Resins: Molecular Weight Distribution, Wetting Behavior, Rheological Properties and Thermal Curing Profiles. *J. Renewable Mater.* **2020**, *8* (6), 603–630.
- (9) Gong, X.; Meng, Y.; Lu, J.; Tao, Y.; Cheng, Y.; Wang, H. A Review on Lignin-Based Phenolic Resin Adhesive. *Macromol. Chem. Phys.* **2022**, *223*, 2100434 DOI: 10.1002/macp.202100434.
- (10) Gao, Z.; Lang, X.; Chen, S.; Zhao, C. Mini-Review on the Synthesis of Lignin-Based Phenolic Resin. *Energy Fuels* **2021**, *35*, 18385–18395.
- (11) Zuo, L.; Yao, S.; Wang, W.; Duan, W. An Efficient Method for Demethylation of Aryl Methyl Ethers. *Tetrahedron Lett.* **2008**, *49* (25), 4054–4056.
- (12) Alonso, M. V.; Oliet, M.; Rodríguez, F.; Astarloa, G.; Echeverría, J. M. Use of a Methylolated Softwood Ammonium Lignosulfonate as Partial Substitute of Phenol in Resol Resins Manufacture. *J. Appl. Polym. Sci.* **2004**, *94* (2), 643–650.
- (13) Chen, Y.; Zhang, H.; Zhu, Z.; Fu, S. High-Value Utilization of Hydroxymethylated Lignin in Polyurethane Adhesives. *Int. J. Biol. Macromol.* **2020**, *152*, 775–785.
- (14) Goncalves, A. R.; Benar, P. hydroxymethylation and Oxidation of Organosolv Lignins and Utilization of the Products. *Bioresour. Technol.* **2001**, *79*, 103–111.
- (15) Chen, X.; Pizzi, A.; Zhang, B.; Zhou, X.; Fredon, E.; Gerardin, C.; Du, G. Particleboard Bio-Adhesive by Glyoxalated Lignin and Oxidized Dialdehyde Starch Crosslinked by Urea. *Wood Sci. Technol.* **2022**, *56* (1), 63–85.
- (16) Ang, A. F.; Ashaari, Z.; Bakar, E. S.; Ibrahim, N. A. Possibility of Enhancing the Dimensional Stability of Jelutong (*Dyera Costulata*) Wood Using Glyoxalated Alkali Lignin-Phenolic Resin as Bulking Agent. *European Journal of Wood and Wood Products* **2018**, *76* (1), 269–282.
- (17) Over, L. C.; Meier, M. A. R. Sustainable Alkylation of Organosolv Lignin with Diallyl Carbonate and Detailed Structural Characterization of Modified Lignin. *Green Chem.* **2016**, *18* (1), 197–207.
- (18) Jawerth, M.; Johansson, M.; Lundmark, S.; Gioia, C.; Lawoko, M. Renewable Thiol-Ene Thermosets Based on Refined and Selectively Allylated Industrial Lignin. *ACS Sustain. Chem. Eng.* **2017**, *5* (11), 10918–10925.
- (19) Jawerth, M. E.; Brett, C. J.; Terrier, C.; Larsson, P. T.; Lawoko, M.; Roth, S. V.; Lundmark, S.; Johansson, M. Mechanical and Morphological Properties of Lignin-Based Thermosets. *ACS Appl. Polym. Mater.* **2020**, *2* (2), 668–676.
- (20) Suota, M. J.; da Silva, T. A.; Zawadzki, S. F.; Sasaki, G. L.; Hansel, F. A.; Paleologou, M.; Ramos, L. P. Chemical and Structural Characterization of Hardwood and Softwood LignoForce Lignins. *Ind. Crops Prod.* **2021**, *173*, No. 114138.
- (21) Matsushita, Y.; Sano, H.; Imai, T.; Fukushima, K. Phenolization of Hardwood Sulfuric Acid Lignin and Comparison of the Behavior of the Syringyl and guaiacyl Units in Lignin. *Journal of Wood Science* **2007**, *53* (1), 67–70.
- (22) Dorrestijn, E.; Laarhoven, L. J. J.; Arends, I. W. C. E.; Mulder, P. The Occurrence and Reactivity of Phenoxy Linkages in Lignin and Low Rank Coal. *J. Anal. Appl. Pyrolysis* **2000**, *54*, 153–192.
- (23) Sherman, M. R.; Williams, L. D.; Sobczyk, M. A.; Michaels, S. J.; Saifer, M. G. P. Role of the Methoxy Group in Immune Responses to Mpeg-Protein Conjugates. *Bioconjug Chem.* **2012**, *23* (3), 485–499.
- (24) Chen, S.; Zhao, Z.; Zhang, Y.; Fang, W.; Lu, J.; Zhang, X. Effect of Methoxy Group Position on Biological Properties of 18F-Labeled Benzyl Triphenylphosphonium Cations. *Nucl. Med. Biol.* **2017**, *49*, 16–23.
- (25) Tanaka, T.; Wakayama, R.; Maeda, S. I.; Mikamiyama, H.; Maezaki, N.; Ohno, H. Unusual Radical Ipso-Substitution Reaction of an Aromatic Methoxy Group Induced by Tris(Trimethylsilyl)Silane-AIBN or SmI₂. *Chem. Commun.* **2000**, *14*, 1287–1288.
- (26) Boto, A.; Hernández, D.; Hernández, R.; Suárez, E. Efficient and Selective Removal of Methoxy Protecting Groups in Carbohydrates. *Tetrahedron Lett.* **2004**, *6* (2), 3785–3788.
- (27) Gadekar, P. K.; Hoermann, M.; Corbo, F.; Sharma, R.; Sarveswari, S.; Roychowdhury, A. Reductive Removal of Methoxyacetyl Protective Group Using Sodium Borohydride. *Tetrahedron Lett.* **2014**, *55* (2), 503–506.
- (28) Yang, H.; Du, Z.; Wang, W.; Song, M.; Sanidad, K.; Sukamtoh, E.; Zheng, J.; Tian, L.; Xiao, H.; Liu, Z.; Zhang, G. Structure-Activity Relationship of Curcumin: Role of the Methoxy Group in Anti-Inflammatory and Anticolic Effects of Curcumin. *J. Agric. Food Chem.* **2017**, *65* (22), 4509–4515.
- (29) Zhang, D.; Yang, G.; Hu, X.; Zhang, Z. Utilization of a Methoxy Group in Lignin to Prepare Amides by the Carbonylation of Amines. *ACS Sustain. Chem. Eng.* **2021**, *9* (35), 11667–11673.
- (30) Mei, Q.; Liu, H.; Shen, X.; Meng, Q.; Liu, H.; Xiang, J.; Han, B. Selective Utilization of the Methoxy Group in Lignin to Produce Acetic Acid. *Angew. Chem.* **2017**, *129* (47), 15064–15068.
- (31) Leiendecker, M.; Hsiao, C. C.; Guo, L.; Alandini, N.; Rueping, M. Metal-Catalyzed Dealkoxylation of Caryl-C Sp³ Cross-Coupling - Replacement of Aromatic Methoxy Groups of Aryl Ethers by Employing a Functionalized nucleophile. *Angewandte Chemie - International Edition* **2014**, *53* (47), 12912–12915.
- (32) Ohno, H.; Wakayama, R.; Maeda, S. I.; Iwasaki, H.; Okumura, M.; Iwata, C.; Mikamiyama, H.; Tanaka, T. Radical Cyclization by Ipso Substitution of the Methoxy Group: Considerable Effect of HMPA on Samarium-Mediated Cyclization. *J. Org. Chem.* **2003**, *68* (15), 5909–5916.
- (33) Wu, Z.; Jiang, H.; Zhang, Y. Pd-Catalyzed Cross-Electrophile Coupling/C-H Alkylation Reaction Enabled by a Mediator generated via C(Sp³)-H Activation. *Chem. Sci.* **2021**, *12* (24), 8531–8536.
- (34) Lapinskaite, R.; Malatinc, Š.; Mateus, M.; Rycek, L. Cross-Coupling as a Key Step in the Synthesis and Structure Revision of the Natural Products Selaginbenzophenones a and b. *Catalysts* **2021**, *11* (6), 708.

- (35) Tobisu, M.; Takahira, T.; Morioka, T.; Chatani, N. Nickel-Catalyzed Alkylated Cross-Coupling of Anisoles with Grignard Reagents via C-O Bond Activation. *J. Am. Chem. Soc.* **2016**, *138* (21), 6711–6714.
- (36) El-Meligy, M. A.; Valachová, K.; Juránek, I.; Tamer, T. M.; Šoltés, L. Preparation and Physicochemical Characterization of Gelatin-Aldehyde Derivatives. *Molecules* **2022**, *27* (2), 7003.
- (37) Ibrahim, A. M.; Shabeer, T. K. Antimicrobial New Schiff Base Polyesters: Design, Thermal, and Structural Characterizations. *Polym. Bull.* **2022**, *79* (2), 1119–1132.
- (38) Yang, W.; Jiao, L.; Wang, X.; Wu, W.; Lian, H.; Dai, H. Formaldehyde-Free Self-Polymerization of Lignin-Derived Monomers for Synthesis of Renewable Phenolic Resin. *Int. J. Biol. Macromol.* **2021**, *166*, 1312–1319.
- (39) Patitungkho, S.; Patitungkho, K. Physicochemical Properties and Biological Activities of Novel Hydrazone Copper Complexes. *Open J. Med. Chem.* **2023**, *13* (01), 1–13.
- (40) An, E. S.; Cho, D. H.; Choi, J. W.; Kim, Y. H.; Song, B. K. Peroxidase-Catalyzed Copolymerization of Syringaldehyde and Bisphenol A. *Enzyme Microb. Technol.* **2010**, *46* (3–4), 287–291.
- (41) Lee, N.; Kim, Y. T.; Lee, J. Recent Advances in Renewable Polymer Production from Lignin-Derived Aldehydes. *Polymers* **2021**, *13* (3), 364.
- (42) Nabipour, H.; Wang, X.; Song, L.; Hu, Y. A High Performance Fully Bio-Based Epoxy thermoset from a Syringaldehyde-Derived Epoxy Monomer Cured by Furan-Derived Amine. *Green Chem.* **2021**, *23* (1), 501–510.
- (43) Tondi, G. Tannin-Based Copolymer Resins: Synthesis and Characterization by Solid State ^{13}C NMR and FT-IR Spectroscopy. *Polymers* **2017**, *9* (6), 223.
- (44) Platt, J. R. Electrochromism, a Possible Change of Color Producing in Dyes by an Electric Field. *J. Chem. Phys.* **1961**, *34*, 862–863.
- (45) Monk, P. M. S.; Mortimer, R. J.; Rosseinsky, D. R. *Electrochromism: Fundamentals and Applications*; John Wiley & Sons 2008.
- (46) Takeuchi, K.; Ishida, S.; Nishikata, T. Dichloromethane as a Chlorination Reagent for α -Bromocarbonyl Compounds in the Presence of a Copper Catalyst. *Chem. Lett.* **2017**, *46* (5), 644–646.
- (47) Tlili, A.; Schranck, J. *The Application of Dichloromethane and Chloroform as Reagents in Organic Synthesis*; Wu, X.-F., Ed.; John Wiley & Sons, 2018. DOI: 10.1002/9783527805624.ch4.
- (48) Mu, M.; Zhang, X.; Yu, G.; Xu, R.; Liu, N.; Wang, N.; Chen, B.; Dai, C. Effective Absorption of Dichloromethane Using Deep Eutectic Solvents. *J. Hazard. Mater.* **2022**, *439*, No. 129666.
- (49) Effenberger, F. Electrophilic Reagents-Recent Developments and Their Preparative Application. *Angew. Chem., Int. Ed.* **1980**, *19*, 151–171.
- (50) Liu, Q.; Zhang, Y.; Zhang, Z.; Liu, T.; Shi, L.; Zhang, G. CH_2Cl_2 as Reagent in the Synthesis of Methylene-Bridged 3,3'-Bis(Oxazolidin-2-One) Derivatives under Ambient Conditions. *RSC Adv.* **2014**, *4* (49), 25933–25939.
- (51) Rudine, A. B.; Walter, M. G.; Wamser, C. C. Reaction of Dichloromethane with Pyridine Derivatives under Ambient Conditions. *J. Org. Chem.* **2010**, *75* (12), 4292–4295.
- (52) Burger, U.; Dreier, F. Reactions of Nitrogen Containing Aromatic Anions with Chlorocarbene. *Tetrahedron* **1983**, *39* (12), 2065–2071.
- (53) Kumar, A. R.; Selvaraj, S.; Jayaprakash, K. S.; Gunasekaran, S.; Kumaresan, S.; Devanathan, J.; Selvam, K. A.; Ramadass, L.; Mani, M.; Rajkumar, P. Multi-Spectroscopic (FT-IR, FT-Raman, ^1H NMR and ^{13}C NMR) Investigations on Syringaldehyde. *J. Mol. Struct.* **2021**, *1229*, No. 129490.
- (54) Chen, S.-W.; Wang, Y.-S.; Hu, S.-Y.; Lee, W.-H.; Chi, C.-C.; Wang, Y.-L. A Study of Trimethylsilane (3MS) and Tetramethylsilane (4MS) Based α -SiCN:H/ α -SiCO:H Diffusion Barrier Films. *Materials* **2012**, *5* (12), 377–384.
- (55) Martínez-Richa, A.; Silvestri, R. L. Developments in Solid-State NMR Spectroscopy of Polymer Systems. In *Spectroscopic Analyses: Developments and Applications*; InTechOpen, 2017; pp 15–30. DOI: 10.5772/intechopen.70116.
- (56) Reif, B.; Ashbrook, S. E.; Emsley, L.; Hong, M. Solid-State NMR Spectroscopy. *Nature Reviews Methods Primers* **2021**, *1*, 1–23.
- (57) Audette, Y.; Congreves, K. A.; Schneider, K.; Zaro, G. C.; Nunes, A. L. P.; Zhang, H.; Voroney, R. P. The Effect of Agroecosystem Management on the Distribution of C Functional Groups in Soil Organic Matter: A Review. *Biol. Fertil. Soils* **2021**, *57*, 881–894.
- (58) Audette, Y.; Longstaffe, J. G.; Gillespie, A. W.; Smith, D. S.; Voroney, R. P. Validation and Comparisons of NaOH and $\text{Na}_4\text{P}_2\text{O}_7$ Extraction Methods for the Characterization of Organic Amendments. *Soil Science Society of America Journal* **2021**, *85* (2), 273–285.
- (59) Yang, J.; Xia, Z.; Kong, F.; Ma, X. The Effect of Metal Catalyst on the Discoloration of Poly(Ethylene Terephthalate) in Thermo-Oxidative Degradation. *Polym. Degrad. Stab.* **2010**, *95* (1), 53–58.
- (60) Gill, P.; Moghadam, T. T.; Ranjbar, B. Differential Scanning Calorimetry Techniques: Applications in Biology and Nanoscience. *J. Biomol. Tech.* **2010**, *21*, 167–193.
- (61) Leyva-Porras, C.; Cruz-Alcantar, P.; Espinosa-Solís, V.; Martínez-Guerra, E.; Piñón-Balderrama, C. I.; Martínez, I. C.; Saavedra-Leos, M. Z. Application of Differential Scanning Calorimetry (DSC) and Modulated Differential Scanning Calorimetry (MDSC) in Food and Drug Industries. *Polymers* **2019**, *12* (1), 5 DOI: 10.3390/polym12010005.
- (62) Kim, S.; Chung, H. Convenient Cross-Linking Control of Lignin-Based Polymers Influencing Structure-Property Relationships. *ACS Sustain. Chem. Eng.* **2023**, *11* (5), 1709–1719.
- (63) Bubnov, A.; Kašpar, M.; Novotná, V.; Hamplová, V.; Glogarová, M.; Kapernaum, N.; Giesselmann, F. Effect of Lateral Methoxy Substitution on Mesomorphic and Structural Properties of Ferroelectric Liquid Crystals. *Liq. Cryst.* **2008**, *35* (11), 1329–1337.
- (64) Yoo, J.; Yang, I.; Kwon, D.; Jung, M.; Kim, M. S.; Jung, J. C. Low-Cost Carbon Xerogels Derived from Phenol-Formaldehyde Resin for Organic Electric Double-Layer Capacitors. *Energy Technol.* **2021**, *9* (4), 2000918 DOI: 10.1002/ente.202000918.